Reactive quenching of electronically excited OH radicals in collisions with molecular hydrogen

David T. Anderson, Michael W. Todd, and Marsha I. Lester

Citation: The Journal of Chemical Physics **110**, 11117 (1999); doi: 10.1063/1.479053
View online: http://dx.doi.org/10.1063/1.479053
View Table of Contents: http://scitation.aip.org/content/aip/journal/jcp/110/23?ver=pdfcov
Published by the AIP Publishing

Reactive quenching of electronically excited OH radicals in collisions with molecular hydrogen

David T. Anderson, Michael W. Todd, and Marsha I. Lester
Department of Chemistry, University of Pennsylvania, Philadelphia, Pennsylvania 19104-6323

(Received 18 March 1999; accepted 12 April 1999)

The hydrogen atom products of the OH $A\,^2\Sigma^+$ $(v=0)+H_2 \rightarrow H+H_2O$ quenching reaction have been characterized by Doppler spectroscopy. The translational energy distribution of the products is bimodal, with the two components accounting for approximately 3% and 40% of the 4.72 eV of available energy. © *1999 American Institute of Physics.* [S0021-9606(99)02123-6]

Collisional deactivation (quenching) of electronically excited OH $A\,^2\Sigma^+$ radicals by molecular partners has received much attention over the past 25 years for both fundamental and practical reasons.[1,2] Collisions facilitate a nonradiative decay process that efficiently removes the OH population from the excited $A\,^2\Sigma^+$ electronic state. The cross sections for collisional quenching of OH $A\,^2\Sigma^+$ by molecular species prevalent in atmospheric and combustion environments have been systematically evaluated in order to account for the effects of quenching on laser-induced fluorescence measurements of OH concentrations based on the OH $A\,^2\Sigma^+ - X\,^2\Pi$ transition.[3–7] The dynamics of this nonadiabatic process have also been studied in weakly bound complexes of OH with H_2, D_2, and N_2.[8–11] To date, however, the products of the electronic quenching event have not been identified experimentally, even for a simple collision partner such as H_2. The OH $A\,^2\Sigma^+ + H_2$ system is particularly interesting since collisional deactivation may proceed by a nonreactive quenching channel that creates ground state OH $X\,^2\Pi$ and H_2 or by a reactive pathway,

$$OH\,A\,^2\Sigma^+ + H_2 \rightarrow H + H_2O. \tag{1}$$

Experimental observation and characterization of the products from this reactive quenching process would provide valuable information on the dynamics of this fundamental nonadiabatic chemical reaction.

Recent *ab initio* calculations of the interaction energy for H_2 with OH in its ground $X\,^2\Pi$ and excited $A\,^2\Sigma^+$ electronic states identified specific orientations that lead to a conical intersection(s) between the ground and excited state adiabatic surfaces.[1] A simplified one-dimensional reaction coordinate based on these calculations is illustrated in Fig. 1. The ground and excited state surfaces are predicted to intersect ~1.4 eV below the OH $A\,^2\Sigma^+ + H_2$ asymptote in a T-shaped H–O–H_2 configuration. For this orientation, the OH $A\,^2\Sigma^+ + H_2$ quenching reaction is shown to be barrierless and, as a result, is expected to occur with an appreciable rate even at low collision energies. The *ab initio* calculations also indicate that the H_2O product will be produced with a large degree of internal excitation due to the significant structural changes that must occur between the conical intersection region and the $H+H_2O$ asymptote.

This Communication demonstrates for the first time that reactive quenching is a significant decay channel for electronically excited OH $A\,^2\Sigma^+$ in collisions with H_2. Doppler spectroscopy is employed to characterize the H atom products, thereby obtaining information on the mechanism and dynamics for reactive quenching of OH by H_2. The kinetic energy distribution of the H atoms reflects the passage of the collision partners through the conical intersection region.

The collision experiments were carried out in a pulsed supersonic expansion. The OH radicals are formed by ArF laser photolysis of fuming HNO_3 (in 30% n-H_2, balance He carrier gas at 150 psi) just beyond the exit of a quartz capillary tube (0.3 mm bore) which is attached to the pulsed valve. Approximately 1000 ns after the photolysis pulse and 2 mm downstream, counterpropagating (parallel polarization) pump and probe lasers intersect the gas pulse. The pump laser (30 mJ, 7 ns, 0.08 cm^{-1}) optically pumps the ground state OH radicals to the $A\,^2\Sigma^+$ electronic state with $v'=0$ and $J'=3/2$ via the $Q_1(1)$ electronic transition near 308 nm.[12] Approximately 20 ns later, the probe beam excites any H atoms that are produced via a two-photon ($2\,^2S \leftarrow\leftarrow 1\,^2S$) transition at 243.1 nm. The resultant Lyman-α fluorescence is detected with a solar blind photomultiplier tube (PMT) after passing through an interference filter.[13,14] The probe beam (12–15 mJ, 4 ns, with an effective two-photon FWHM of 0.5 cm^{-1}) is generated by frequency doubling in BBO the output (~486 nm) of the signal beam of a BBO optical parametric oscillator. Both the pump and probe beams are gently focused with 50 cm focal length lenses. The output of the PMT is preamplified and monitored via gated detection.

The 193 nm photolysis of HNO_3 in H_2/He carrier gas, which is used to generate the OH radicals, also produces H atoms. These ''background'' H atoms presumably originate from direct photolysis[15] of HNO_3 as well as from reaction of ground state OH with H_2 in the high-density region of the expansion where photolysis occurs.[9,10] The background H atoms are cooled substantially in the supersonic expansion before they reach the probe laser interaction region. The Doppler profile of the background H atoms is well fit by a Gaussian function with a FWHM of 0.75 cm^{-1}, corresponding to a translational temperature of ≈150 K. Based on this translational temperature and an 11 $Å^2$ cross section for

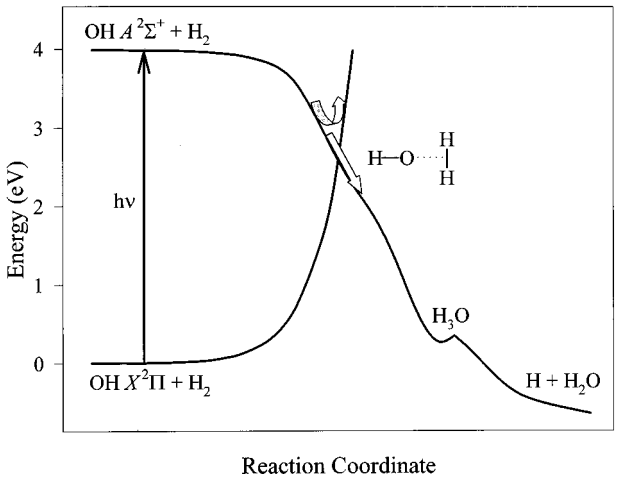

FIG. 1. Simplified potential energy surface for H_2 interacting with OH in its ground $X\,^2\Pi$ and excited $A\,^2\Sigma^+$ electronic states (adapted from Ref. 1), revealing a conical intersection in the T-shaped HO–H_2 orientation. Two pathways exit from the conical intersection; the nonreactive quenching pathway follows down to OH $X\,^2\Pi + H_2$ and the reactive pathway generates $H+H_2O$ after passing through the H_3O intermediate. Collisions of electronically excited OH $A\,^2\Sigma^+$ ($h\nu$) with H_2 result in quenching via direct or indirect passage (stylized arrows) through the conical intersection region.

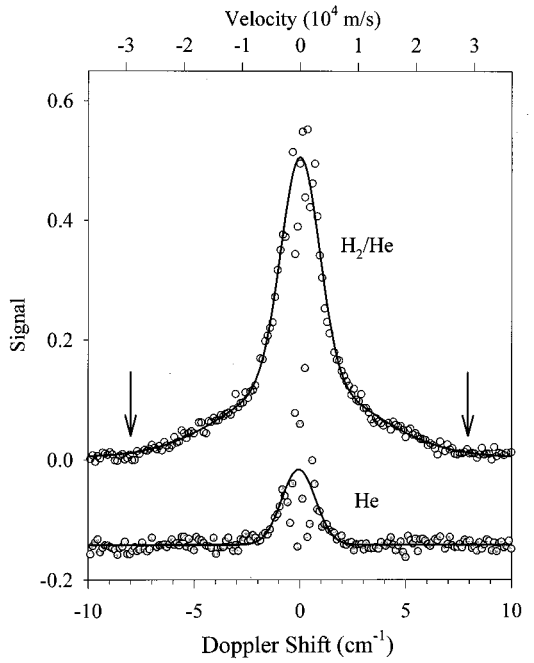

FIG. 2. Doppler profiles for product H atoms on the two-photon $2\,^2S \leftarrow \leftarrow 1\,^2S$ transition at $v_0 = 82\,259\ cm^{-1}$ and corresponding H atom velocities. (Upper trace) Pump-induced H atom signal arising from reactive quenching of OH $A\,^2\Sigma^+$ ($v'=0$, $J'=3/2$) in H_2/He carrier gas. The arrows indicate the calculated energetic limit for the Doppler shift. (Lower trace) Significantly reduced pump-induced H atom signal in pure He carrier gas. The increased scatter in the pump-induced signals at small Doppler shifts results from subtraction of the large H atom background signal (probe laser only, FWHM $=0.75\ cm^{-1}$). Solid lines are fits to the experimental data.

electronic quenching,[7] the electronically excited OH $A\,^2\Sigma^+$ radicals are estimated to undergo ~1 collision with H_2 in the 20 ns pump–probe delay.

In order to study the H atoms produced by reactive quenching in the presence of the background H atoms, a standard pump laser ON–OFF subtraction scheme was utilized in the data acquisition. This was implemented by operating the pump laser at half the repetition rate of the probe laser. On alternating pulses, the H atom signal arising from the combination of both pump and probe lasers or that resulting from the probe laser only (background) is collected and then subtracted from one another. A typical pump-induced H atom Doppler profile in a H_2/He carrier gas is presented in Fig. 2. At line center (v_0), the pump-induced (i.e., subtracted) H atom signal is ~10% of the background signal.

To make sure that the pump-induced signal arises from reactive quenching of OH $A\,^2\Sigma^+$ by H_2, a number of internal checks have been conducted. First, no subtracted signals are observed if the 193 nm photolysis laser is turned off. Second, if the pump laser is detuned from the OH $Q_1(1)$ line, no pump-induced signals are detected. However, analogous pump-induced H atom Doppler profiles are observed when the pump laser is tuned to OH $P_1(1)$ and $R_1(1)$ lines. Third, experiments have been carried out in a pure He carrier gas, also shown in Fig. 2, where a substantially reduced (~eightfold) pump-induced signal is found. The small signal in He is presumably due to reactive quenching of OH $A\,^2\Sigma^+$ with a component of the HNO_3 sample. Finally, the pump-induced H atom signal disappears if the pump–probe laser interaction region is moved downstream into the collision free region of the expansion. Thus, the source of the pump-induced H atom signal in H_2/He carrier gas is ascribed to reactive quenching collisions of OH $A\,^2\Sigma^+$ with H_2.

The observed H atom Doppler profile is consistent with the energetics of the quenching reaction. The total available energy for the $H+H_2O$ products is readily calculated,

$$E_{\mathrm{AVL}} = E_{h\nu} - \Delta H_{\mathrm{rxn}} + E_{\mathrm{col}}, \tag{2}$$

where $E_{h\nu} = 4.025\,\mathrm{eV}$, $\Delta H_{\mathrm{rxn}} = -0.64\,\mathrm{eV}$ for the ground state reaction,[16] and $E_{\mathrm{col}} \approx 0.05\,\mathrm{eV}$. Based on conservation of linear momentum and energy, the maximum velocity of the H atom product is obtained using

$$v_{\mathrm{H}}^{\mathrm{max}} = \sqrt{\frac{2E_{\mathrm{AVL}}}{m_{\mathrm{H}}(1 + m_{\mathrm{H}}/m_{\mathrm{H_2O}})}}. \tag{3}$$

This yields $v_{\mathrm{H}}^{\mathrm{max}} = 29\,250$ m/s and corresponds to a maximum Doppler shift of $\pm 8.03\ cm^{-1}$. The Doppler shift (Δv_{D}) is linearly related to the H atom velocity (v_{H}), $\Delta v_{\mathrm{D}} = v_0 v_{\mathrm{H}}/c$. The experimental Doppler profile extends out to the calculated energetic limit, which is indicated by arrows in Fig. 2.

The observed H atom Doppler profile is a one-dimensional projection of the three-dimensional velocity distribution along the propagation axis of the probe laser beam. The H atom velocity distribution is expected to be spatially isotropic since it results from binary collisions of OH $A\,^2\Sigma^+$ with H_2 that average over the impact parameter and relative orientations of the collision partners. The experimental Doppler profile is best represented by a sum of two Gaussian functions, shown in Fig. 2, with the quality of the least squares fit demonstrating that the data is well modeled by

TABLE I. Parameters derived from the H atom product Doppler profiles: the breadth (FWHM), the translational temperature (T), the average H atom translational energy $\langle E_{T,H}\rangle$, the average energy released into product translational energy $\langle E_T\rangle$, and the fraction of the 4.72 eV of available energy deposited in translation of the products $\langle f_T\rangle$.

FWHM[a] (cm^{-1})	T (K)	$\langle E_{T,H}\rangle$ (eV)	$\langle E_T\rangle$ (eV)	$\langle f_T\rangle$
1.78(35)[b]	920(350)	0.12(4)	0.13(4)	0.028(8)
6.62(56)	12700(2100)	1.65(27)	1.74(29)	0.37(6)

[a]The probe laser bandwidth (0.5 cm^{-1}) does not influence the fitted Doppler width.

[b]The uncertainties reflect one standard deviation for a complete set of 15 measurements, not the quality of an individual fit.

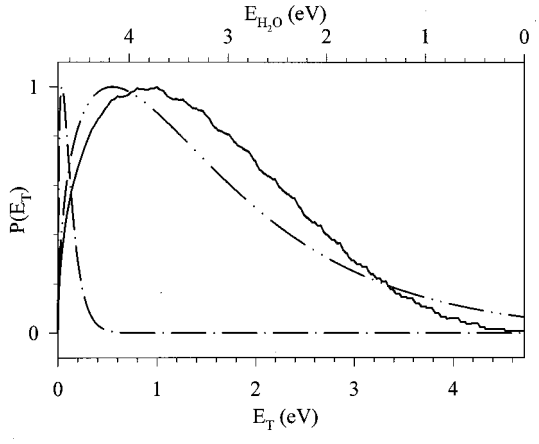

FIG. 3. The translational energy distribution $P(E_T)$ calculated for the T=920 K (dotted-dashed) and 12 700 K (dotted–dotted–dashed) H atom translational temperatures. The peak of each distribution has been normalized to 1. The upper axis displays the corresponding internal energy of the H_2O fragment. The $P(E_T)$ calculated using the statistical model (solid) compares favorably with the broader experimental distribution.

this analytical form. The bimodal Doppler profile indicates that two different H atom velocity distributions result from reactive quenching of OH $A\,^2\Sigma^+$ in collisions with H_2.

The velocity distribution of the nascent H atoms may be thermalized to some extent prior to detection since this process is known to have a large cross section (10 $Å^2$) for energetic H atoms in a He bath gas.[17] Doppler profiles recorded at pump–probe delays as great as 100 ns, however, showed no statistically significant difference from short time measurements. While some relaxation may occur in the 20 ns pump–probe delay, particularly for faster moving H atoms, thermalization is *not* expected to produce a bimodal velocity distribution.

A translational temperature[18] can be derived from each component of the Doppler profile by using the fitted FWHM and assuming a Boltzmann translational energy distribution

$$T=\frac{(\mathrm{FWHM}/2v_0)^2 m_H c^2}{2k\ln 2}. \tag{4}$$

The results are summarized in Table I. If the integrated areas of the two Gaussian functions are assumed to be proportional to the H atom number density, then 60% of the H atoms are produced with an average translational temperature of nearly 13 000 K and the remaining 40% with a temperature of approximately 1000 K. The average translational energy of the H atom, $\langle E_{T,H}\rangle = 3kT/2$, is readily evaluated and used to calculate the total translational energy released into product translation via linear momentum conservation, $\langle E_T\rangle = m_{H_3O}/m_{H_2O}\langle E_{T,H}\rangle$. Therefore, the fraction of energy released into translational energy of the products for the narrow and broad Doppler widths is calculated to be $\langle f_T\rangle = 0.028$ and 0.37, respectively. Conservation of energy dictates that H_2O is produced with a bimodal internal energy distribution, with corresponding average internal energies of 4.59 eV and 2.99 eV.

The high degree of internal excitation in the H_2O products can be understood from previous theoretical calculations of this nonadiabatic reaction. The geometry at the conical intersection is known from *ab initio* calculations at the CASSCF level of theory.[1] The conical intersection has C_{2v} symmetry with an intermolecular bond length of $R(\text{O-c.m.H}_2)=1.45$ Å. This configuration means that directly after the OH $A\,^2\Sigma^+ + H_2$ partners pass through the conical intersection, the newly formed H_2O will have bond lengths of $r_{OH_1}=1.03$ Å and $r_{OH_2}=1.5$ Å as well as an HOH angle of 165°. Therefore, the nascent H_2O product should be highly vibrationally excited (asymmetric stretch and bend) since H_2O has a very different equilibrium structure ($r_{OH}=0.96$ Å and HOH=105°).[19]

The internal excitation of the H_2O product is not sufficient to result in dissociation of the nascent H_2O product because the bond energy,[19] $D_0(\text{H–OH})=5.113$ eV, exceeds the available energy by almost 0.5 eV. This channel being energetically closed, the present data poses an obvious question: Why a bimodal velocity distribution for the H atom products?

The bimodal distribution most likely arises from the passage of the reactants through the conical intersection region.[20–24] For some OH $A\,^2\Sigma^+ + H_2$ collisions, the collision partners may evolve directly through the conical intersection region in a single pass. This ''direct'' reaction would involve a nonadiabatic transition near the conical intersection, followed by motion on the ground state reactive potential energy surface. Since the H_2O product is expected to be highly vibrationally excited, the fraction of the available energy deposited into translational energy of the products would be minimal. On the other hand, if the collision partners were to miss the conical intersection on the first approach, the reactants could become momentarily trapped in the deep adiabatic well of the upper electronic state, permitting energy to be redistributed among the available HO–H_2 vibrational degrees of freedom. Eventually, the HO–H_2 collision complex would funnel through the conical intersection region and produce H+H_2O. In this case, there would be a more statistical distribution of energy among the H_2O vibrational degrees of freedom and the H atom would depart with a greater fraction of the available energy.

Alternatively, the bimodal velocity distribution may arise from the HO–H_2 collision pair evolving through two distinct angular regions of the conical intersection. Yarkony[25] has predicted that two different structures in the

vicinity of the conical intersection lead to $H+H_2O$ (Fig. 7 of Ref. 25). One has a nuclear configuration reminiscent of an early transition state for an abstraction reaction, while the other appears to be analogous to a late transition state structure for an insertion reaction. Passage through these distinct regions could yield very different product state distributions.

Finally, the observed translational energy distributions are compared with a statistical model. The product translational energy distribution, $P(E_T)$, can be calculated using the fitted translational temperatures according to

$$P(E_T)dE_T=\frac{2}{\pi^{1/2}(kT)^{3/2}}E_T^{1/2}e^{-E_T/kT}dE_T. \tag{5}$$

This calculation assumes a Maxwell–Boltzmann distribution of product speeds. The $P(E_T)$ for the two components of the Doppler profile are plotted in Fig. 3. Assuming a statistical distribution of final states, $P(E_T)$ can also be modeled from the vibrational state density $N(E)$ of the H_2O product ($\omega_1=3750\,\mathrm{cm}^{-1}$, $\omega_2=3650\,\mathrm{cm}^{-1}$, $\omega_3=1600\,\mathrm{cm}^{-1}$) and the three-dimensional translational density of states for the recoiling products, $P(E_T)=N(E)E_T^{1/2}$. The statistical calculation, also plotted in Fig. 3, predicts $\langle E_T\rangle=1.50\,\mathrm{eV}$ or $\langle f_T\rangle=0.32$. While agreement with experiment is not quantitative, or expected to be, this simple model qualitatively reproduces the component associated with the faster and broader $P(E_T)$. By contrast, the slower translational energy distribution is not consistent with the statistical model and corresponds to a highly excited H_2O product with a very narrow distribution of internal energies.

This paper demonstrates that reactive quenching is a significant decay channel for low energy collisions of electronically excited $OH\,A\,^2\Sigma^+$ ($v=0$) with H_2. The Doppler profile of the H atom products is bimodal, indicating that the H atoms are produced with two distinct kinetic energy distributions. The bimodal distribution originates from two different dynamical pathways through the conical intersection that funnels $OH\,A\,^2\Sigma^+ + H_2$ into $H+H_2O$. Ongoing experimental work is attempting to shed further light on the mechanism for this nonadiabatic reaction through isotopic substitutions and H/D atom detection. Further theoretical calculations are also needed to explore the dynamics of this fundamental electronic quenching reaction.

This work has been supported by the Office of Basic Energy Sciences of the Department of Energy, with partial equipment support from the Chemistry Division of the National Science Foundation. The authors thank Bethany V. Pond for her assistance in the early stages of the experiments and S. P. Walch for conducting the *ab initio* calculations.

[1] M. I. Lester, R. A. Loomis, R. L. Schwartz, and S. P. Walch, J. Phys. Chem. **101**, 9195 (1997).
[2] D. R. Crosley, J. Phys. Chem. **93**, 6273 (1989).
[3] K. H. Becker, D. Haaks, and T. Tartarczyk, Chem. Phys. Lett. **25**, 564 (1974).
[4] P. Hogan and D. D. Davis, J. Chem. Phys. **62**, 4574 (1975).
[5] K. R. German, J. Chem. Phys. **64**, 4065 (1976).
[6] I. S. McDermid and J. B. Laudenslager, J. Chem. Phys. **76**, 1824 (1982).
[7] R. A. Copeland, M. J. Dyer, and D. R. Crosley, J. Chem. Phys. **82**, 4022 (1985).
[8] L. C. Giancarlo and M. I. Lester, Chem. Phys. Lett. **240**, 1 (1995).
[9] R. A. Loomis and M. I. Lester, J. Chem. Phys. **103**, 4371 (1995).
[10] R. A. Loomis, R. L. Schwartz, and M. I. Lester, J. Chem. Phys. **104**, 6984 (1996).
[11] R. L. Schwartz, L. C. Giancarlo, R. A. Loomis, R. T. Bonn, and M. I. Lester, J. Chem. Phys. **105**, 10224 (1996).
[12] G. H. Dieke and H. M. Crosswhite, J. Quant. Spectrosc. Radiat. Transf. **2**, 97 (1961).
[13] T. W. Hänsch, S. A. Lee, R. Wallenstein, and C. Wieman, Phys. Rev. Lett. **34**, 307 (1975).
[14] H. Umemoto, T. Nakae, H. Hashimoto, K. Kongo, and M. Kawasaki, J. Chem. Phys. **109**, 5844 (1998).
[15] T. L. Myers, N. R. Forde, B. Hu, D. C. Kitchen, and L. J. Butler, J. Chem. Phys. **107**, 5361 (1997).
[16] M. Alagia, N. Balucani, P. Casavecchia, D. Stranges, G. G. Volpi, D. C. Clary, A. Kliesch, and H.-J. Werner, Chem. Phys. **207**, 389 (1996).
[17] J. Park, N. Shafer, and R. Bersohn, J. Chem. Phys. **91**, 7861 (1989).
[18] R. N. Zare and D. R. Herschbach, Proc. IEEE **51**, 173 (1963).
[19] G. Herzberg, *Electronic Spectra of Polyatomic Molecules* (Van Nostrand, New York, 1966).
[20] Similar ideas regarding the dynamics through a conical intersection have been suggested in the photodissociation of NH_3 (Refs. 21, 22) and the reaction of Na^*+H_2 (Ref. 23).
[21] L. J. Butler and D. M. Neumark, J. Phys. Chem. **100**, 12801 (1996).
[22] M. N. R. Ashfold, R. N. Dixon, M. Kono, D. H. Mordaunt, and C. L. Reed, Philos. Trans. R. Soc. London, Ser. A **355**, 1659 (1997).
[23] T. J. Martinez, M. Ben-Nun, and R. D. Levine, J. Phys. Chem. **101**, 6389 (1997).
[24] D. R. Yarkony, Acc. Chem. Res. **31**, 511 (1998).
[25] D. R. Yarkony, J. Phys. Chem. **100**, 18612 (1996).